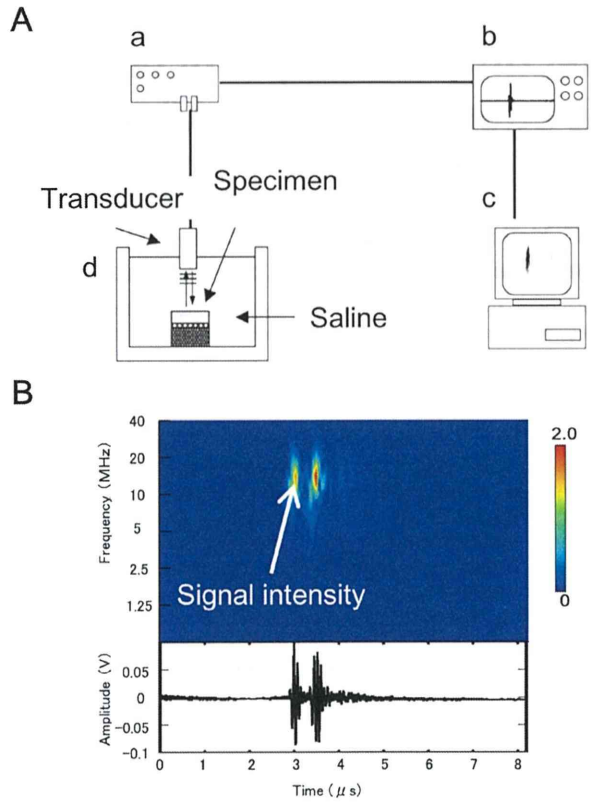

Figure 1. A scheme of the ultrasound measurement system. A) The ultrasound measurement system consists of a transducer, a pulser/receiver (a), a digital oscilloscope (b), and a personal computer (c), and saline bath and probe (d). B) typical A-mode echogram (lower) and its wavelet map (upper) of the cartilage. Each diagram has 2 peaks. The left one is a reflex echo from the surface, and the right one is from the subchondral bone. The wavelet map provides comprehensive information on the transient distribution of the intensity and frequency of an echo wave. US signal intensity is shown by graduation on the wavelet map.
doi:10.1371/journal.pone.0089484.g001

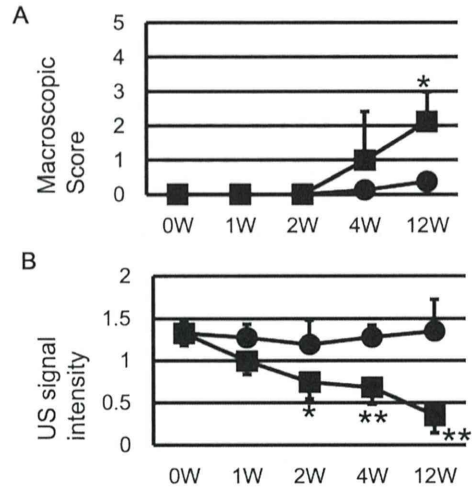

Figure 2. US signal intensity detected the deterioration of rabbit cartilages ahead of the macroscopic change. A) Macroscopic score of sham and ACLT side showed significant difference only at 12 weeks. B) US signal intensity of ACLT side decreased overtime and had significant difference to the sham side as early as 2 weeks. *: $p<0.05$ to sham side. **: $p<0.01$ to sham side.
doi:10.1371/journal.pone.0089484.g002

Materials and Methods

Ethics Statement

All animal studies were conducted in accordance with principles by Kyoto University Committee of Animal Resources, based on International Guiding Principles for Biomedical Research Involving Animals. All procedures for this study were approved by Kyoto University Committee of Animal Resources (Permit Number: Med Kyo 10184). For all human species, ethical approval for this study was granted by the ethics committee of Kyoto University Graduate School and Faculty of Medicine. Written informed consent was provided and obtained from all study participants.

Animal Samples

Eighteen skeletally matured female Japanese white rabbits (weight, 4.0–4.5 kg) were used. Two rabbits (4 knees) were allocated to 0-week control, and 4 were randomly allocated into 4 groups that were examined at 1, 2, 4, or 12 weeks after surgery. They were individually housed at 22°C and 50% humidity with a 14/10-h light/dark cycle and had free access to food and water. For operations, intravenous pentobarbital sodium (25 mg/kg) was used to induce and maintain general anesthesia. An intraarticular injection (3 mL) of 1% lidocaine to each knee was used and a medial parapatellar incision was made to expose both knee joints. Bilateral anterior cruciate ligaments were exposed, and left anterior cruciate ligament transection (ACLT) was carefully performed. The joint capsule and skin incision were closed. The rabbits were allowed full weight-bearing postoperatively. The animals were sacrificed by an intravenous injection of pentobarbital sodium (100 mg/kg) and were macroscopically evaluated by two orthopaedic surgeons. In brief, cartilage changes were graded on a scale from 0 to 5 (0, intact surface normal in appearance; 1, minimal fibrillation; 2, overt fibrillation, distinguished surface irregularity, or cracks; 3, erosion from 0 to 2 mm; 4, erosion from 2 to 5 mm; 5, erosion >5 mm) [8]. The cartilage samples were stored at −20°C before use.

Human Samples

Human articular cartilage samples were obtained from a series of total knee arthroplasties of OA. Patients were diagnosed as OA according to the criteria of the American College of Rheumatology [9]. The KL grading system was used to score knees [10]. The cartilage of the weight-bearing area of the lateral femoral condyle was graded, using the International Cartilage Repair Society (ICRS) grading system by two experienced orthopaedic surgeons [11]. Patients were included in the study only when there was an ICRS grade 0 lesion in the weight-bearing area of the lateral femoral condyle. Eventually, three males and 17 females (mean age, 73.9 years; range, 55–82) (10 patients with KL grade 3 and 10 patients with KL grade 4) were involved in this study. One cylindrical osteochondral plug (diameter, 6 mm) for each patient was harvested from the center of the ICRS grade 0 lesion. The cartilage samples were stored at −20°C before use.

Ultrasound Evaluation

The ultrasonic measurement system with noncontact probe has been described previously and provides a quantitative assessment of tissues properties [5,12,13]. In brief, the transducer is 3 mm in

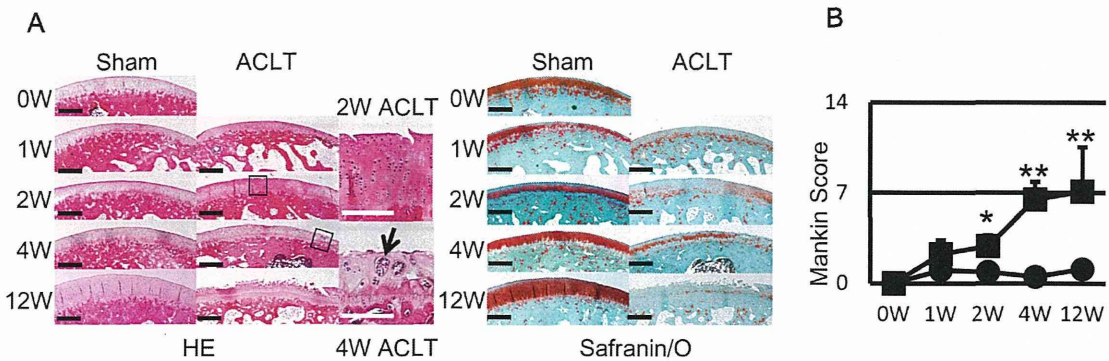

Figure 3. Histological sections and Mankin score of rabbit cartilages also showed OA change at 2 weeks. A) OA change such as fibrillation of the surface and decrease of safranin/O stainingwas detected from 2 weeks and deteriorated overtime. At 12 weeks, most of samples clearly showed OA change with fissures and further decrease of safranin/O staining. In HE, Black boxes of 2W and 4W ACLT side are showed in right column. Black arrow indicates the cloning of chondrocytes. D) Mankin score of ACLT side increased overtime and there was significant difference after 2 weeks, like US signal intensity. Black bar in histology indicates 100 μm and white bar indicates 50 μm. *: $p<0.05$ to sham side. **: $p<0.01$ to sham side.

doi:10.1371/journal.pone.0089484.g003

diameter, and the center frequency of the ultrasonic signal is 10 MHz (Figure 1A). While examining cartilage, 2 large-amplitude groups of reflected waves are observed: one is from the cartilage surface and the other is from the subchondral bone (Figure 1B). The maximum magnitude of the wave reflected from the articular cartilage surface on the wavelet map was defined as US signal intensity. Each animal specimen was examined at 3 different sites: at the center, and 5 mm anterior and posterior to the center of the weight-bearing area. Each measurement was performed twice, and data from the 3 points were averaged. Each human specimen was examined at the center of the cylindrical osteochondral plug; each measurement was performed twice, and the average value was used.

Histological Analysis

Samples were fixed in 4% paraformaldehyde. Animal and Human samples were decalcified with 0.25 mol/L ethylenediaminetetraacetic acid in phosphate-buffered saline solution (pH 7.4) and Morse's solution (10% sodium citrate and 22.5% formic acid), respectively. Sagittal sections (6-μm thick) were cut, stained with hematoxylin and eosin (HE) and safranin O/fast green (safranin/O). Histological scoring of the cartilage was performed by two blinded investigators and averaged by using the Mankin scoring system with the following 4 categories: cartilage structure (6 points), cartilage cells (3 points), staining (4 points), and tidemark integrity (2 points); normal and severely degenerated cartilage scoring 0 and 14, respectively [14]. Referring to the classification of Mankin and his colleagues, human specimens were classified into 4 stages based on their Mankin scores: nearly normal (0≤ Mankin score <2), early OA (2≤ Mankin score <6), moderate OA (6≤ Mankin score <10), and late OA (10≤ Mankin score ≤14) [15,16].

FTIRI Evaluation

FTIRI was used to determine the spatial distribution of proteoglycan and collagen. The paraffin sections were mounted on metal plates and deparaffinized. A Fourier transform infrared spectrometer (FT-IR-460 PLUS, JASCO, Tokyo) coupled to a microscope (Intron-IRT-30, JASCO, Tokyo) was used for data acquisition. Spatial pixel size was 20×20 μm. Spectral resolution was set to 4 cm^{-1} wavenumber, and a spectral region of 2000~670 cm^{-1} was collected. An integrated absorbance area of the carbohydrate region (1150–950 cm^{-1}) and that under the amide I peak (1710–1595 cm^{-1}) were defined as the proteoglycan and collagen contents, respectively [17,18]. Two slices were evaluated for each cartilage and the averaged collagen and proteoglycan contents of the superficial zone and whole cartilage were used for quantitative analysis.

Statistical Analysis

All values are means ± standard deviation. Student's *t*-test was used for comparing sham and ACLT sides in the animal study. One-way ANOVA with a post hoc comparison was used to analyze differences among OA stages in the human study. Pearson's linear correlation coefficient was used to determine correlations between the ultrasound and FTIRI parameters. Spearman's correlation coefficient was used to determine correlations between the ultrasound parameter and Mankin scores. Statistical significance was set at $P<0.05$.

Results

Animal Specimens

The sham side of the LFC showed little OA-like changes throughout the experimental period. At 1 or 2 weeks, there was no visible change at the LFC in the ACLT side. At 4 weeks, some rabbits exhibited slight LFC fibrillation in ACLT side. At 12 weeks, most rabbits exhibited fibrillation at the LFC of ACLT side. The macroscopic scores of the LFC were significantly higher only at 12 weeks (Figure 2A).

Ultrasound Evaluation (Figure 2B)

The US signal intensity of the ACLT side decreased with time. At 2 weeks, the US signal intensity of ACLT (0.74±0.20) was significantly lower than that of sham (1.19±0.29). At 4 and 12 weeks, the US signal intensity of the LFC (0.68±0.20 and 0.34±0.21, respectively) decreased further and was significantly lower than sham side (1.28±0.14 and 1.35±0.37, respectively).

Histological Evaluation (Figure 3A)

At one week, both the ACLT and sham sides showed reduced safranin/O staining. At 2 weeks, although the safranin/O staining

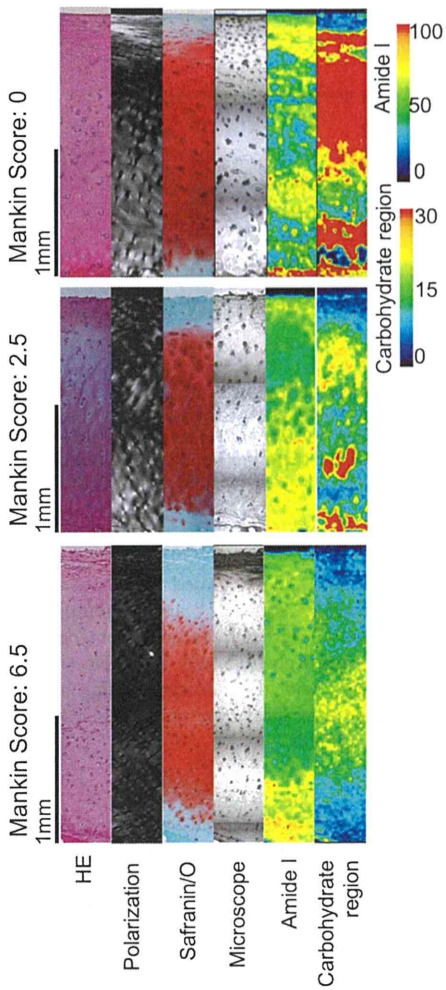

Figure 4. Though gross surface appearance was similar, histology section showed variety of OA stages. Histological section of the representative samples of each stage. HE, poralized microscope of HE, Safranin/O, Microscope for FTIR region of interest, Amide I mapping of FTIR and Carbohydrate region mapping of FTIR are shown. Upper panel is patient 1, middle is patient 2 and lower is patient 7. Black bar indicate 1 mm. Nearly normal cartilage showed a smooth surface, superficial collagen fiber network parallel to the surface, dense Safranin/O staining, Amid I rich area in superficial layer and Carbohydrate region rich areas in whole layer. As cartilage degeneration, these findings disappear or decrease.
doi:10.1371/journal.pone.0089484.g004

of the sham side looked restored, the surfaces of the ACLT group appeared crackled and the safranin/O staining was not restored, and started to show OA-like changes. At 4 weeks, the safranin/O staining of the sham side was completely restored. The ACLT side exhibited fibrillation of the cartilage surface and chondrocyte cloning. At 12 weeks, the sham side appeared normal, whereas the ACLT side exhibited progression of OA-like changes, including fibrillation increase, chondrocyte cloning, and decrease in safranin/O staining. The Mankin scores (Figure 3B) of the ACLT side continuously increased and the Mankin scores of both sides were significantly different at 2, 4 and 12 weeks.

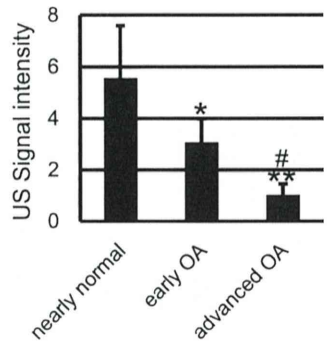

Figure 5. US signal intensity of macroscopically intact human specimens was considerably different among 3 histological stages. US signal intensity of the nearly normal cartilage was significantly higher than that of early OA or moderate OA cartilage. There was also difference between early OA and moderate OA. *: $p<0.05$ to nearly normal stage. **: $p<0.01$ to nearly normal stage. #: $p<0.05$ to early OA stage. ##: $p<0.01$ to early OA stage.
doi:10.1371/journal.pone.0089484.g005

Human Specimens

Two specimens were excluded due to unsuccessful decalcification process of the paraffin sections. Mankin scores ranged widely (0 to 8), although all samples were obtained from ICRS grade 0 sites. The samples were classified into the following stages: nearly normal (3 samples), early OA (12 samples), and moderate OA (3 samples). There were no samples which were classified as late stage.

Histological Evaluation (Figure 4)

Samples in the nearly normal stage had smooth surface, dense safranin/O staining, and columnar chondrocyte arrangements. FTIRI mapping showed Amide I rich area in superficial zone and Carbohydrate region rich area along with Safranin/O staining. In the early OA stage, samples showed slight fibrillation and reduced safranin/O staining and its amide I and carbohydrate region rich area decreased. In the moderate OA stage, fibrillation became obvious and chondrocyte arrangement became random, safranin/O staining decreased, and the amide I or carbohydrate rich area was not seen.

Ultrasound Evaluation (Figure 5)

US signal intensity of the nearly normal stage was significantly higher than early or moderate stage, and US signal intensity of early stage was significantly higher than moderate stage.

Table 1. Correlation of Mankin Score and its subcategories with US signal intensity.

	Correlation with US signal Intensity	
	correlation coefficient	P value
Mankin Score	−0.80	<0.001
I. structure	−0.72	0.002
II. cells	−0.67	0.004
III. Safranin/O staining	−0.58	0.01
IV. Tidemark	−0.42	0.06

doi:10.1371/journal.pone.0089484.t001

Table 2. Correlation of Amide I and Carbohydrate region value with US signal intensity.

		Correlation with US signal Intensity	
		correlation coefficient	P value
Amide I value	superficial zone	0.82	<0.001
	whole zone	0.06	0.80
Carbohydrate region value	superficial zone	0.74	<0.001
	whole zone	0.61	0.006

doi:10.1371/journal.pone.0089484.t002

Correlation with Ultrasound Parameter

US signal intensity was significantly correlated with Mankin scores and its sub categories, including structure, cells, and safranin/O staining, but not tidemark (Table 1). There was a strong correlation between US signal intensity and the amide I value of the superficial zone. On the other hand, there was no significant correlation between US signal intensity and the amide I values of the whole zone (Table 2). Meanwhile, there was a significant correlation between US signal intensity correlated to carbohydrate region values of both the whole zone and the superficial zone, and correlation with the superficial zone was greater than that of whole zone (Table 2).

Discussion

The US signal intensity was able to detect macroscopically undetectable OA changes in both animal and human samples. In the animal part, there were no macroscopic changes in the ACLT side at 2 weeks; however, the US signal intensity of the ACLT side was already lower than that of the sham side. The histological Mankin scores also showed degenerative changes in the sham side at 2 weeks. Although all the human samples appeared intact, some samples were histologically degenerated. There was a significant difference among the US signal intensity of nearly normal, early OA, and moderate OA samples.

In the animal study, the US signal intensity detected cartilage deterioration when changes could only be identified histologically. OA changes were not macroscopically identified until 4 weeks after ACLT. However, upon histological evaluation, changes in OA, such as tiny crackle on the cartilage or decreased safranin/O staining, were observed at 2 weeks. Thus, ultrasound differentiated changes at this early stage.

In the human samples, although all cartilage samples were obtained from macroscopically intact areas (ICRS grade 0), Mankin scores varied widely. Three moderate OA samples out of 20 were actually diagnosed as normal by a trained orthopaedic surgeon. In clinical situations, orthopaedic surgeons mainly diagnose cartilage changes macroscopically. Thus, evaluating articular cartilage solely based on external findings is unreliable and more objective and distinct decision standards are required. We think US signal intensity with noncontact probe is possible candidate for objective evaluation of cartilage quality.

In human species, the correlation between US signal intensity and the subcategory of Mankin score showed the strongest correlation with structure which was largely from the superficial layer information but no correlation with tidemark which was from the information of deep region. US signal intensity was also strongly correlated with the amide I value of the superficial zone, but not with the whole zone. In terms of the correlation between US signal intensity and carbohydrate region value, correlation of superficial zone was greater than that of whole zone. The correlation of ultrasound reflection to collagen or proteoglycan content is previously reported [19,20,21]. Moreover, we and other groups reported that the reflected ultrasound waves provide superficial information of the cartilage [19,22,23]. The numerical analysis of ultrasonic propagation in articular cartilage from another study of our group suggests that the collagen content from the surface to one wave length (1600[m/s]/10 MHz = 0.16 mm) is correlated with US signal intensity [24]. Since the depth of the superficial zone was ~100 μm, the information of the superficial zone was included in the depth of ultrasonic propagation. The depth of rabbit cartilage was 100–200 μm, which was adequate for our evaluation device. Thus, these correlations with the superficial zone information shows that US signal intensity reflect the cartilage degeneration of superficial zone.

There are some disagreement concerning the use of US signal intensity [25,26], as US signal intensity cannot directly measure any intrinsic physical characteristics. However, we have found a strong correlation between US signal intensity and some clinically important elements of the cartilage. Moreover, the present study revealed that ultrasound can detect macroscopically undetectable change in OA. Our ultimate goal is to improve the diagnostic use of arthroscopic ultrasound systems in order to detect early degeneration in human articular cartilage.

Although the current study demonstrates clinically important findings, it has some limitations. First, the number of animals and human samples is limited. In the human study, only 20 samples were evaluated, which is too small for analyzing subgroups including gender or age. Second, instead of biochemical analysis, FTIRI with univariate-based spectral analysis was used to evaluate cartilage and determine the spatial distribution of materials of interest including collagen and proteoglycan. Amide I and carbohydrate lesion values were used to measure collagen and proteoglycan, respectively, although we did not determine their actual amounts. Nowadays, it is reported that multivalent analysis provides more accurate concentration revealing subtle change [27]. In this study, even with a simple univariate data analysis, we could find the surface change in human OA cartilage. Third, the precise qualitative analysis of the type of collagen was not performed; amide I reflects the total amount of collagen but cannot distinguish its type. Type-II collagen is predominant in articular cartilage, and we obtained a strong correlation between amide I and type-II collagen in OA cartilage in the pretest [28]. Therefore, we believe the data mainly represent changes in type-II collagen, but the data for amide I involves type-I and other minor collagen types. Finally, our current method of ultrasound evaluation could not be performed from the outside of the skin. We believe that our method is less- invasive because of the availability during arthroscopic surgery using non-contact probe, however this methods is not non-invasive. In parallel with the further accumulation of the basic information, we think it

important to improve the method so as to evaluate and quantitate the cartilage from the skin surface.

In conclusion, we showed the ability of ultrasound to distinguish microscopic OA change in both animal and human cartilage, especially reflecting the information of the degeneration of superficial zone. We believe that the ultrasound is a potential method for diagnosing early subtle changes in OA at the preclinical stage.

Acknowledgments

The authors thank to Dr. Ko Yasura, Dr. Yukihiro Okamoto and Dr. Mikiko Miura for their technical help and valuable discussion.

Author Contributions

Conceived and designed the experiments: KN MK YN. Performed the experiments: KN T. Shirai T. Satake. Analyzed the data: KN MK HK. Contributed reagents/materials/analysis tools: HK KM SN RA TN SM. Wrote the paper: KN MK.

References

1. Felson DT (2006) Clinical practice. Osteoarthritis of the knee. N Engl J Med 354: 841–848.
2. Van Dyck P, Kenis C, Vanhoenacker FM, Lambrecht V, Wouters K, et al. (2013) Non-invasive imaging of cartilage in early osteoarthritis. Bone Joint J; 95: 738–746.
3. Kiviranta P, Lammentausta E, Toyras J, Kiviranta I, Jurvelin JS (2008) Indentation diagnostics of cartilage degeneration. Osteoarthritis Cartilage 16: 796–804.
4. Hattori K, Ikeuchi K, Morita Y, Takakura Y (2005) Quantitative ultrasonic assessment for detecting microscopic cartilage damage in osteoarthritis. Arthritis Res Ther 7: R38–46.
5. Nishitani K, Nakagawa Y, Gotoh T, Kobayashi M, Nakamura T (2008) Intraoperative acoustic evaluation of living human cartilage of the elbow and knee during mosaicplasty for osteochondritis dissecans of the elbow: an in vivo study. Am J Sports Med 36: 2345–2353.
6. Nishitani K, Shirai T, Kobayashi M, Kuroki H, Azuma Y, et al. (2009) Positive effect of alendronate on subchondral bone healing and subsequent cartilage repair in a rabbit osteochondral defect model. Am J Sports Med 37 Suppl 1: 139S–147S.
7. Kuroki H, Nakagawa Y, Mori K, Kobayashi M, Nakamura S, et al. (2009) Ultrasound properties of articular cartilage immediately after osteochondral grafting surgery: in cases of traumatic cartilage lesions and osteonecrosis. Knee Surg Sports Traumatol Arthrosc 17: 11–18.
8. Wang SX, Laverty S, Dumitriu M, Plaas A, Grynpas MD (2007) The effects of glucosamine hydrochloride on subchondral bone changes in an animal model of osteoarthritis. Arthritis Rheum 56: 1537–1548.
9. Altman R, Asch E, Bloch D, Bole G, Borenstein D, et al. (1986) Development of criteria for the classification and reporting of osteoarthritis. Classification of osteoarthritis of the knee. Diagnostic and Therapeutic Criteria Committee of the American Rheumatism Association. Arthritis Rheum 29: 1039–1049.
10. Kellgren JH, Lawrence JS (1957) Radiological assessment of osteo-arthrosis. Ann Rheum Dis 16: 494–502.
11. Kleemann RU, Krocker D, Cedraro A, Tuischer J, Duda GN (2005) Altered cartilage mechanics and histology in knee osteoarthritis: relation to clinical assessment (ICRS Grade). Osteoarthritis Cartilage 13: 958–963.
12. Mori K (2002) Measurement of the mechanical properties of regenerated articular cartilage using wavelet transformation. Vol. 6, 6 ed. Tokyo: Elsevier 133–142 p.
13. Kuroki H, Nakagawa Y, Mori K, Ohba M, Suzuki T, et al. (2004) Acoustic stiffness and change in plug cartilage over time after autologous osteochondral grafting: correlation between ultrasound signal intensity and histological score in a rabbit model. Arthritis Res Ther 6: R492–504.
14. Mankin HJ, Dorfman H, Lippiello L, Zarins A (1971) Biochemical and metabolic abnormalities in articular cartilage from osteo-arthritic human hips. II. Correlation of morphology with biochemical and metabolic data. J Bone Joint Surg Am 53: 523–537.
15. Ehrlich MG, Houle PA, Vigliani G, Mankin HJ (1978) Correlation between articular cartilage collagenase activity and osteoarthritis. Arthritis Rheum 21: 761–766.
16. Murata M, Trahan C, Hirahashi J, Mankin HJ, Towle CA (2003) Intracellular interleukin-1 receptor antagonist in osteoarthritis chondrocytes. Clin Orthop Relat Res 409: 285–95.
17. Camacho NP, West P, Torzilli PA, Mendelsohn R (2001) FTIR microscopic imaging of collagen and proteoglycan in bovine cartilage. Biopolymers 62: 1–8.
18. Boskey A, Camacho NP (2007) FT-IR imaging of native and tissue-engineered bone and cartilage. Biomaterials 28: 2465–2478.
19. Kuroki H, Nakagawa Y, Mori K, Kobayashi M, Yasura K, et al. (2006) Maturation-dependent change and regional variations in acoustic stiffness of rabbit articular cartilage: an examination of the superficial collagen-rich zone of cartilage. Osteoarthritis Cartilage 14–8: 784–792.
20. Hattori K, Takakura Y, Tanaka Y, Habata T, Kumai T, et al. (2006) Quantitative ultrasound can assess living human cartilage. J Bone Joint Surg Am 88 Suppl 4: 201–212.
21. Saarakkala S, Laasanen MS, Jurvelin JS, Torronen K, Lammi MJ, et al. (2003) Ultrasound indentation of normal and spontaneously degenerated bovine articular cartilage. Osteoarthritis Cartilage 11: 697–705.
22. Hattori K, Uematsu K, Matsumoto T, Ohgushi H (2009) Mechanical effects of surgical procedures on osteochondral grafts elucidated by osmotic loading and real-time ultrasound. Arthritis Res Ther 11: R134.
23. Viren T, Saarakkala S, Kaleva E, Nieminen HJ, Jurvelin JS, et al. (2009) Minimally invasive ultrasound method for intra-articular diagnostics of cartilage degeneration. Ultrasound Med Biol 35: 1546–1554.
24. Mori K, Nakagawa Y, Kuroki H, Ikeuchi K, Nakashima K, et al. (2006) Non-Contact Evaluation for Articular Cartilage Using Ultrasound. JSME International Journal, series A 49: 242–249.
25. Saarakkala S, Jurvelin JS, Zheng YP, Nieminen HJ, Toyras J (2007) Quantitative information from ultrasound evaluation of articular cartilage should be interpreted with care. Arthroscopy 23: 1137–1138.
26. Zheng YP, Huang YP (2008) More intrinsic parameters should be used in assessing degeneration of articular cartilage with quantitative ultrasound. Arthritis Res Ther 10: 125.
27. Kobrina Y, Rieppo L, Saarakkala S, Pulkkinen HJ, Tiitu V, et al. (2013) Cluster analysis of infrared spectra can differentiate intact and repaired articular cartilage. Osteoarthritis Cartilage 21: 462–469.
28. Nishitani K, Kobayashi M, Nakagawa Y, Nakamura T (2011) Detection of early degeneration of osteoarthritis cartilage by evaluating collagen content with Fourier transform infrared imaging and ultrasound. The journal of Japanese Society of Clinical Sports Medicine 19: 258–264 in Japanese.

Knee Surg Sports Traumatol Arthrosc (2014) 22:2635–2640
DOI 10.1007/s00167-013-2506-z

KNEE

Improved design decreases wear in total knee arthroplasty with varus malalignment

Kazutaka Nishikawa · Ken Okazaki · Shuichi Matsuda · Yasutaka Tashiro · Shinya Kawahara · Hiroyuki Nakahara · Shigetoshi Okamoto · Takeshi Shimoto · Hidehiko Higaki · Yukihide Iwamoto

Received: 17 August 2012 / Accepted: 9 April 2013 / Published online: 16 April 2013
© Springer-Verlag Berlin Heidelberg 2013

Abstract
Purpose Controversy still exists whether coronal malalignment would influence the long-term survival of total knee arthroplasty (TKA). The hypothesis was that an improved design of the articular surface of modern TKA would prevent the increase in contact stresses and thus decrease the wear even when the implant was placed in a varus position. Two different designs of TKA were compared biomechanically and clinically.
Methods The patients whose prosthesis was initially placed in a varus alignment by the postoperative long-leg radiographs were selected. Seventeen knees using the NexGen LPS and 16 knees using the MG I were examined. Changes in postoperative alignment and the thickness of the polyethylene insert in a follow-up period of approximately 7 years were evaluated. Additionally, an in vitro biomechanical testing was conducted to measure the contact stresses and the contact area at the tibiofemoral joint of the NexGen LPS and the MG I components mounted on a servohydraulic testing device.
Results Although the long-leg alignment did not change in NexGen LPS, the varus alignment significantly progressed in MG I. The thickness of polyethylene insert in MG I decreased a significantly greater amount compared with that in NexGen LPS. Biomechanical test showed that the NexGen LPS had a larger contact area and lower mean and peak contact stresses than the MG I significantly.
Conclusion These results suggest that comprehensive factors of modern prosthesis including improved implant designs could improve the durability of polyethylene insert and decrease implant failures due to component malalignment.

Keywords Total knee arthroplasty (TKA) · Design · Alignment · Wear · Contact stress

K. Nishikawa · K. Okazaki (✉) · S. Matsuda · Y. Tashiro · S. Kawahara · H. Nakahara · S. Okamoto · Y. Iwamoto
Department of Orthopaedic Surgery, Graduate School of Medical Sciences, Kyushu University, 3-1-1 Maidashi, Higashi-ku, Fukuoka 812-8582, Japan
e-mail: okazaki@med.kyushu-u.ac.jp

T. Shimoto · H. Higaki
Department of Biorobotics, Faculty of Engineering, Kyushu Sangyo University, 2-3-1 Matsukadai, Higashi-ku, Fukuoka 813-8503, Japan

Introduction

Total knee arthroplasty (TKA) is a successful treatment for the pain and decreased function of knee osteoarthritis. The success of TKA depends on restoration of limb alignment, accurate implant positioning and optimal gap balancing [10, 11]. Several studies reported that the survival rate of TKA is improved if leg alignment is restored between 3° of valgus and varus on the mechanical axis [19]. Therefore, surgeons have set a goal to achieve a postoperative limb alignment closer to the mechanical axis.

Postoperative optimal alignment, however, remains a matter of debate. A recent study reported that postoperative limb alignment is not related to implant survival even at 15 years postoperatively from a modern TKA [2, 14, 16]. One of the possible reasons is that improved implant designs decrease the risk of wear problems even with malalignment of the component. We previously reported that a varus-aligned TKA resulted in an increased propensity toward varus alignment and affected the wear of the ultra-high-molecular-weight polyethylene (UHMWPE) when the "flat-on-flat" design in the coronal plane was

used [12]. However, the results of varus-aligned "curved-on-curved" implant TKAs, which theoretically do not increase contact stresses even with malalignment, are unknown. As far as we know, no study has been reported regarding the comparison of polyethylene wear of two different designs of TKA implanted in varus alignment with both clinical and biomechanical aspects.

This study compared the influence of varus alignment on the UHMWPE between two designs of TKA biomechanically and clinically. In biomechanical testing, we evaluated the effect of tibial tilt on the contact stresses of the MG I (flat-on-flat) and the NexGen (curved-on-curved) systems. In the clinical study, we selected the patients whose prosthesis was initially implanted in varus alignment and compared the changes of coronal alignment and joint space in time between these designs. We hypothesized that the curved design would not significantly increase contact stresses with varus tilting in the biomechanical testing and that the varus alignment would less worsen with the curved design than with the flat-on-flat design in the clinical study.

Materials and methods

NexGen LPS

Between September 1999 and March 2006, 173 consecutive patients (223 knees) underwent TKA with the NexGen Legacy Posterior Stabilized (LPS) Fixed Bearing Knee System (Zimmer, Warsaw, IN) at our hospital. The NexGen LPS system features curved-on-curved weight-bearing surface with polyethylene insert made from Himont 1900 resin (H1900) (Himont, Wilmington, Delaware). The initial postoperative coronal alignment was evaluated with full-length weight-bearing anteroposterior (AP) radiographs for 76 knees in which the correct AP radiograph was obtained in more than a 2-year follow-up. Forty-one knees were excluded because the full-length weight-bearing AP radiograph at the follow-up was not taken in a correct AP direction. The weight-bearing ratio (WBR) was measured as described below. To select the patients who had varus alignment at the initial postoperative radiograph, 18 knees whose WBR was more than 50 % (valgus alignment) were excluded. As a result, 16 patients with 17 knees who had varus alignment were enrolled in the study. The medical records and radiological data for all patients were reviewed retrospectively. There were 3 men and 13 women, and the mean patient age at operation was 69.5 ± 9.9 years. The mean preoperative BMI was 25.6 ± 3.3 kg/m^2. All patients were retired. The pathologies determined in the diagnoses were osteoarthritis in 12 knees and rheumatoid arthritis in 5 knees. All TKAs were implanted using conventional guides, with an intramedullary femoral system and extramedullary tibial system. All the tibial components were cemented and the femoral components were cemented in 8 knees and fixed with a cementless manner in 9 knees. The mean follow-up period was 7.3 ± 1.7 years. The follow-up evaluation was based on radiographic examinations. Radiological assessment involved full-length weight-bearing AP radiographs as well as standard AP and lateral radiographs.

MG I

Between October 1987 and January 1990, 39 consecutive patients (54 knees) underwent TKA with the Miller-Galante (MG) I Knee System (Zimmer, Warsaw, IN) at our hospital. The MG I system features flat-on-flat weight-bearing surface with polyethylene insert made from H1900 (Himont, Wilmington, Delaware). A radiographic assessment of 20 of these knees has been reported previously [12]. Similarly, the patients whose knees on the initial postoperative radiographs were in a neutral or valgus position had been excluded. This left 13 patients with 16 knees to be enrolled in the study. The medical records and radiological data for all patients were reviewed retrospectively. The patients included 1 male and 12 females. All patients had osteoarthritis, and the mean age at operation was 70.6 ± 3.7 years. The mean preoperative BMI was 26.0 ± 2.9 kg/m^2. All patients were retired. All TKAs were implanted using conventional guides, with an intramedullary femoral system and an extramedullary tibial system. All but two knees had the femoral and tibial components fixed without cement. Cement was used to fix only the femoral component in one knee and to fix both the tibial and the femoral components in one knee. The mean follow-up period was 7.5 ± 2.0 years. The follow-up evaluation was based on radiographic examinations. Radiological assessment involved full-length weight-bearing AP radiographs as well as standard AP and lateral radiographs.

Polyethylene inserts in both groups were with UHMWPE, which was not cross-linked and made from the same material (H1900).

Radiographic assessment

A mechanical axis of each extremity was defined by a straight line drawn from center of the femoral head to the center of the talus (Fig. 1). The WBR was calculated by measuring the distance from the medial edge of the proximal tibia to the point where the mechanical axis intersects the proximal tibia, and then dividing that measurement by the entire width of the proximal tibia (Fig. 2). A percentage was calculated by multiplying this ratio by 100 %. Femoral (α) and tibial (β) joint line angles were also measured on full-length radiographs. The shortest perpendicular distance from the lower edge of the tibial tray to the femoral component was measured. This distance was assumed to be the thickness

of the UHMWPE insert where the femoral component makes contact with the tibial component in extension. Magnification error was corrected by the true mediolateral size of the metal tibial tray, and wear for the medial components of the knee prosthesis was calculated. In the MG I group, the analog radiographic films were used for measurement. The WBR, α angle, β angle and the liner thickness were measured by a goniometer and an electronic ruler. In the NexGen LPS group, printings of the films, which were saved on DICOM data, were used and the WBR, α angle and β angle were measured in the same way. The liner thickness was measured by the SYNAPSE OP-A (FUJIFILM, Japan). Excluding the knees with inadequate films in which the X-ray did not parallel the joint line, this distance was measured in the remaining 16 knees using the NexGen LPS and 13 MG I knees. The changes in WBR, the α and β angles, the wear rate, and the thickness of the UHMWPE of the NexGen LPS were compared to those of the MG I. Portions of this data have been previously published [12].

Biomechanical study

Contact stresses at the tibiofemoral joint were measured in the NexGen and the MG I components. In the coronal plane, the NexGen femoral component has a curved surface with a small radius that matches the radius of curvature on the conforming tibial surface. On the other hand, the MG I adopts a flat configuration on both the femoral and tibial surfaces in the coronal plane. The femoral and tibial components were mounted to a servohydraulic testing device with specially designed fixtures. A digital electronic pressure sensor (K-Scan sensor; Tekscan Inc., Boston, Mass) was placed at the implant interface to measure tibiofemoral contact area and stresses [13]. A compressive load of 2,058 N was applied to each knee system at 15° and 90° of flexion with 0° of tilt in the mediolateral direction. A force three times the body weight (2,058 N) was applied because gait analyses have shown that a tibiofemoral force is 3.0 times the body weight for level walking. Contact area and stress measurements were made five times with the components seated normally. Femoral components were then tilted 5° toward varus, changed into this new position with a vice, and all tests were repeated five times.

This study was approved by the institutional review board (Kyushu University, 3-1-1 Maidashi, Higashi-ku, Fukuoka 812-8582, Japan, No. 21-8).

Statistical analysis

In the radiographic study, statistical analyses for comparison of parameters on radiographs of MG I and NexGen LPS at the initial follow-up and final follow-up were performed with the Mann–Whitney U test. Statistical analysis for comparison of the difference of changes of parameters on radiographs between the MG I and NexGen LPS was performed with the Mann–Whitney U test. In the biomechanical study, statistical analyses were performed with a non-paired t test. The level of $p < 0.05$ was considered to be significant.

Fig. 1 Mechanical axis was defined by the use of full-length weight-bearing AP radiographs

A power analysis was performed to estimate the required sample size in each group. To achieve 80 % power ($\alpha = 0.05$), the estimated sample size in each group was 13 knees.

Intraobserver and interobserver repeatability of measurements of α angle, β angle, WBR and the thickness of UHMWPE

In the evaluation of intraobserver repeatability, the intraclass correlation coefficients for the α angle, β angle, WBR

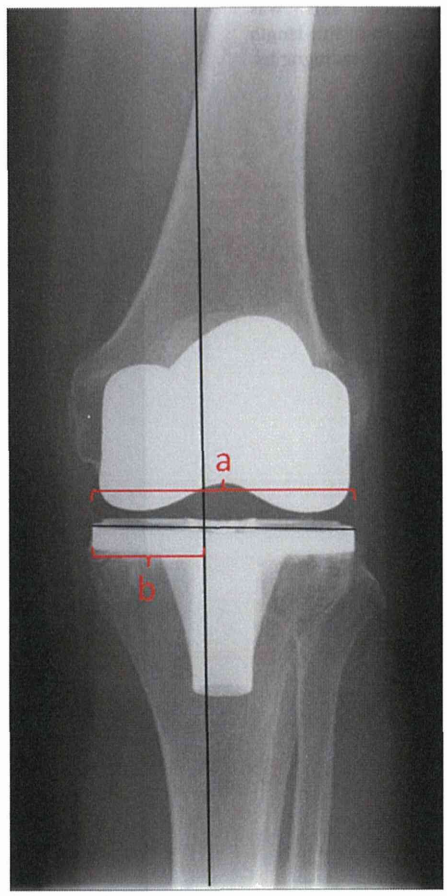

Fig. 2 Limb alignment was measured by drawing a mechanical axis on each limb depicted in a full-standing radiograph. The location where the mechanical axis intersects the tibial plateau is expressed as a percentage of tibial width (weight-bearing ratio = $b/a \times 100$ %)

and the thickness of UHMWPE were 0.94, 0.81, 0.96 and 0.99, respectively. The interclass correlation coefficient was calculated from the data of the measurements of two of the observers (HN, SK) and the average of the three measurements of the other observer (KN). The interclass correlation coefficients for α angle, β angle, WBR and the thickness of UHMWPE were 0.81, 0.80, 0.95 and 0.99, respectively.

Results

Radiographic study

For the patients with the NexGen LPS, the WBR, α angle, β angle and thickness of UHMWPE did not change significantly during the postoperative period (Table 1). For the patients with MG I, the WBR, β angle and thickness of the UHMWPE were significantly decreased (Table 2). The changes per year of WBR, α angle and β angle of NexGen LPS were −0.41 %, −0.04° and −0.004°, respectively. These same measurements in MG I were −1.36 %, 0.05° and −0.15°, respectively. They did not differ significantly between the NexGen LPS and MG I. Polyethylene inserts of MG I were all 8.5 mm. The size of polyethylene insert of NexGen LPS was 10 mm in 6 knees, 12 mm in 8 knees, 14 mm in 2 knees and 17 mm in 1 knee. The thickness of the MG I UHMWPE (−0.14 mm/year) decreased more significantly compared with the NexGen LPS (−0.01 mm/year) ($p = 0.006$).

Biomechanical study

When the knee was flexed at both 15° and 90° with 0° of tilt, the NexGen LPS (251.3, 168.7 mm^2) had a larger contact area than the MG I (168.7, 144.8 mm^2) ($p < 0.001$). The NexGen LPS (8.2, 12.2 MPa) had lower mean contact stresses than the MG I (12.5, 14.2 MPa) ($p < 0.001$). Peak contact stresses with 0° tilt of NexGen LPS were lower than those of MG I significantly (Fig. 3). When the femoral component was tilted to 5° varus, the entire compressive load transferred to the medial condyle. At both 15° and 90° flexion, the NexGen LPS and MG I had smaller contact areas (189.7, 132.3 mm^2/89.4, 73.5 mm^2) and higher mean contact stresses (10.9, 15.6 MPa/23.1, 28.0 MPa) than those with 0° of tilt. Also, the NexGen LPS had a larger contact area and lower mean stresses than the MG I ($p < 0.001$). Peak stresses with a tilted tibia of MG I were more than twice those of NexGen LPS (Fig. 4).

Discussion

The most important finding of the present study was that thickness of UHMWPE of MG I which was initially aligned in varus position decreased significantly compared with that of NexGen LPS also aligned in varus position, indicating that the curved-on-curved surface design adopted in NexGen improved durability against wear of UHMWPE compared with the flat-on-flat design of MG I even though being implanted in varus alignment. Biomechanical study supported this findings showing that UHMWPE with flat configurations (MG I) had very high contact stresses due to edge loading. Many studies reported that high contact stress increases polyethylene wear [5, 6, 8, 9]. Since both of MG I and NexGen used the same material for UHMWPE in this series, less contact stress due to the improved design is considered to be the main factor that contributed to the less wear of UHMWPE of NexGen.

Restoration of a neutral mechanical axis, accurate implant positioning and optimal gap balancing are requirements for a

Table 1 Radiographic measurement of the NexGen LPS at postoperative and at final follow-up periods

	Initial follow-up	Final follow-up	*p* value
Weight-bearing ratio (%)	37.6 ± 8.1	35.0 ± 8.6	n.s.
α angle (°)	95.2 ± 2.0	95.1 ± 2.0	n.s.
β angle (°)	88.7 ± 1.4	88.5 ± 1.7	n.s.
Thickness of UHMWPE (mm)	11.0 ± 1.7	10.9 ± 1.7	n.s.

Table 2 Radiographic measurement of MG I at postoperative and at final follow-up periods

	Initial follow-up	Final follow-up	*p* value
Weight-bearing ratio (%)	34.3 ± 8.0	24.2 ± 11.4	0.003
α angle (°)	96.5 ± 2.3	96.6 ± 2.9	n.s.
β angle (°)	88.3 ± 1.6	87.2 ± 1.5	0.002
Thickness of UHMWPE (mm)	8.5 ± 0.5	7.9 ± 0.5	0.002

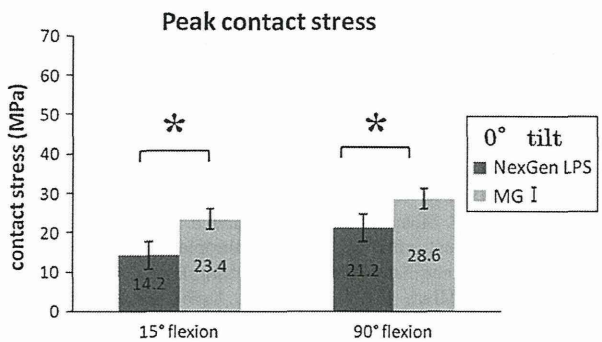

Fig. 3 Peak contact stresses with 0° varus tilt with the NexGen LPS and MG I at 15° and 90° flexion. *The difference between MG I and NexGen LPS is significant ($p < 0.05$)

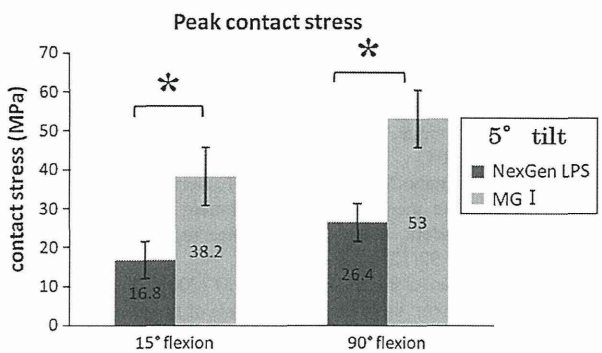

Fig. 4 Peak contact stresses with 5° varus tilt with the NexGen LPS and MG I at 15° and 90° flexion. *The difference between MG I and NexGen LPS is significant ($p < 0.05$)

successful TKA [1, 10, 11]. Therefore, surgeons have set a goal to achieve a postoperative limb alignment closer to the mechanical axis. Postoperative optimal alignment, however, has been the subject of controversy due to the recent reports that postoperative limb alignment is not related to implant survival 15-year postoperatively from a modern TKA [2, 14, 16]. We thought that one of the reasons is that improved implant designs decrease the risk of implant failure even with malalignment of the component; therefore, biomechanical and clinical studies were conducted comparing two different designs of TKA.

In addition to the wear problem, the major failure modes of TKA are tibial collapse and ligamentous instability [7, 15, 17, 21]. Ritter et al. [20] reported that varus malalignment was associated with a 5.9 times greater risk of failure due to medial collapse than neutral overall alignment. In our study, the β angle of the knees using MG I decreased during the follow-up period and the change in the β angle of MG I tends to be larger than that of the NexGen LPS ($p = 0.08$). The decrement in the β angle indicates progression of tibial medial collapse. However, the difference was very small and the method of stem fixation varied in each. The MG I used four pegs and the NexGen LPS adopts one central stem for tibial fixation. This study could not conclude that improvement in surface design decreased progression of tibial medial collapse.

The coronal alignment of initially varus-aligned TKA using MG I worsened to become toward more varus. On the other hand, coronal alignment of varus-aligned TKA using NexGen LPS did not change significantly during the follow-up period. The changes in WBR tend to differ between the NexGen LPS and MG I ($p = 0.09$). This change in alignment was caused by many factors, such as wear of the UHMWPE, ligamentous instability and subsidence of the tibial component. In this study, the change in WBR would be a combined effect of the wear of UHMWPE and subsidence of the tibial component. However, the effect of ligamentous instability on the change of WBR is unknown because we did not measure ligamentous tension intraoperatively and postoperatively.

There were several limitations in this study. First, our study was limited by its retrospective design. However,